

STRUCTURAL ANALYSIS OF THE JET TAE ANTENNA

P. H. Titus¹, J. Snipes¹, A. F. Fasoli^{2,1}, D. Testa², B. Walton³, and JET-EFDA contributors

¹MIT Plasma Science and Fusion Center, 185 Albany St. Cambridge MA 02139 titus@psfc.mit.edu

²Centre de Recherches en Physique des Plasmas, Association Euratom - Confédération Suisse, Ecole Polytechnique Fédérale de Lausanne, CH-1015 Lausanne, Switzerland

³Euratom/UKAEA Fusion Association, Culham Science Center, Abingdon, UK

In this paper the mechanical design of the new active MHD antennas for JET is described and the structural/mechanical analysis for the antennas is presented. These new antennas replace the existing $n = 1$ or 2 saddle coils with a set of eight smaller antennas designed to excite Toroidal Alfvén Eigenmodes (TAE's) with high toroidal mode number ($n \sim 10$) in the frequency range of 30 kHz - 500 kHz. TAE's with these higher mode numbers are expected in ITER and could enhance the loss of fast alpha particles in a burning plasma regime. By studying the properties of stable TAE's excited actively by these antennas, high performance regimes of operation avoiding unstable fast particle driven modes can be found. A more complete overview of the experiment may be found in Reference[1] Two antenna assemblies will be installed at toroidally opposite positions. Antenna wires are protected from the plasma heat flux by CFC tiles mounted on mini-limiters, located between the individual windings. The main structural element is a box section. The support scheme utilizes cantilevered brackets that connect to the saddle coils, and "wing" brackets which add support to the top of the frame. Conservative estimates of the disruption currents in the MHD antennas and frame were used to calculate loading and resulting stress in the antenna structure. Fields, field transients, and halo current specifications were provided by JET. The frame originally was designed as a continuous loop, and was converted to an open structure to break eddy current loops. Antenna eddy currents were computed assuming the antenna is shorted. In the final design, frame forces primarily result from halo currents entering around the mini limiters that now protect the antenna windings. Accelerations due to the vessel disruption dynamic response were included in the loading. The antenna mechanical design has been shown to perform adequately for all identified disruption loading.

I. INTRODUCTION

Design details have evolved. An antenna module consists of four rectangular windings of 4 mm Inconel 718 wire, with 18 turns, wound on ceramic spool pieces. The main structural element is a 60 X 120mm Inconel 625 SST box

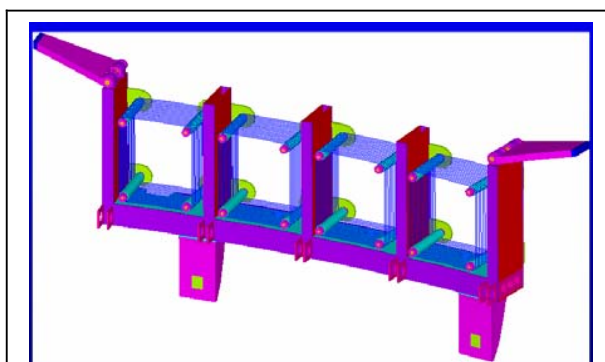


Fig. 1. March 2004 Structural Model - Resistive Earths 2 Milliohm Top and 3 Milliohm Bottom. This is a front view, or view from the plasma.

section. The support scheme utilizes cantilevered brackets that connect to the saddle coils, and "wing" brackets which add support to the top of the frame. The ANSYS model used to qualify the antenna is shown in Figure 1. Figure 2 shows the analysis model of an earlier design which had many weaknesses that the later design sought to

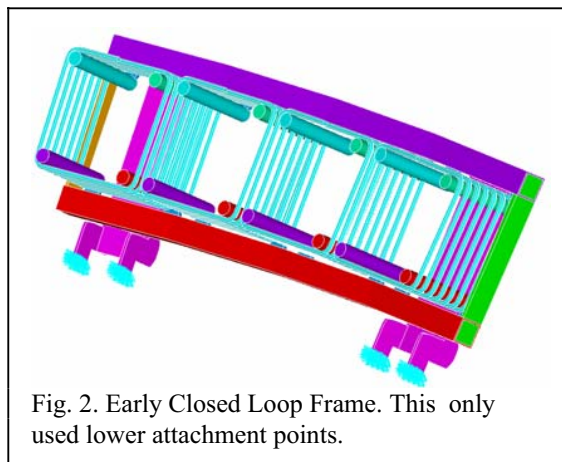


Fig. 2. Early Closed Loop Frame. This only used lower attachment points.

correct.

I OPERATING ENVIRONMENT

I.A. Halo Currents

In the earliest designs, halo current loads were calculated assuming the full inventory of halo current crossed the toroidal field and passed downward the full

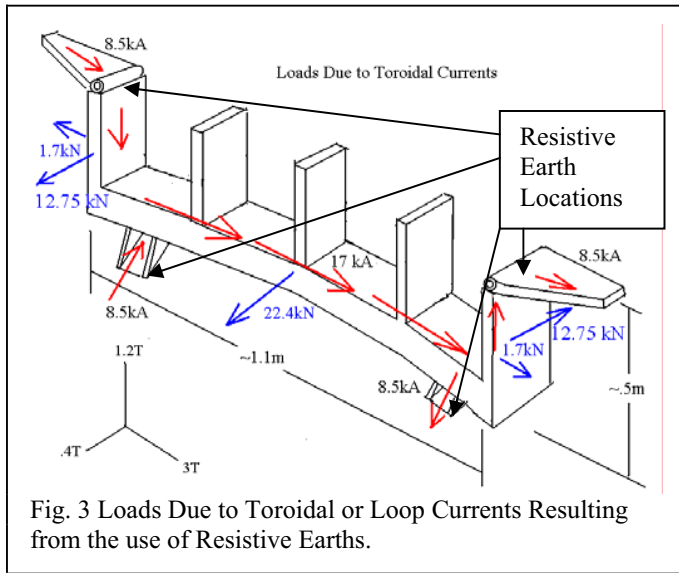


Fig. 3 Loads Due to Toroidal or Loop Currents Resulting from the use of Resistive Earths.

height of the frame to the lower attachment points. To improve the loading, the attachment points were connected to their mounting locations through resistive straps which have resistances sized to produce currents that minimize net loading. With the addition of resistive earths at the four attachment points, a small toroidal current crossed with the poloidal field component is added but the much larger loading due to poloidal currents crossed with toroidal field is much reduced. In the next treatment of the halo currents, the 90kA inventory of halo Currents was split evenly between the five mini-limiter vertical frame elements. In the last analyses these were shifted to four of the verticals to one side to more properly model the shadowing of the plasma. Halo currents were specified for this analysis by JET [3]. The assumed halo current distribution in the antenna is shown in Figure 4.

I.B. Poloidal Fields and field changes during a diorsruption

Table 1 Poloidal Field and it's Rate of Change During a Disruption

| Location | Parallel (T) | Perp. (T) | Parallel (T/sec) | Parallel Decay Time | Perp. (T/sec.) | Perp. Decay Time |
|------------------|--------------|-----------|------------------|-------------------------|----------------|-----------------------|
| Poloidal Limiter | 1.2 | .4 | 120 | 2.5e-3 sec. (or 10e-3?) | 80 | 5e-3 sec. (or 10e-3?) |
| Outer Wall | 1.2 | .4 | 70 | | 10 | |

These form the basis of eddy loop currents, and are used for calculating currents in the antenna wire and box sections. The main box currents are shown in Figure 5

and 6 Additionally there is a toroidal current resulting connection of the antenna frame to the vessel.

I.C. Toroidal Currents Resulting from Connection to the Vessel

During a disruption there is a loop current around whole machine driven by an 800 V loop voltage. So there is a 50 V or 100 V potential across the antenna depending on the position of poloidal limiters' own earth. The limiters actually straddle octant sector joints. The sector joints,

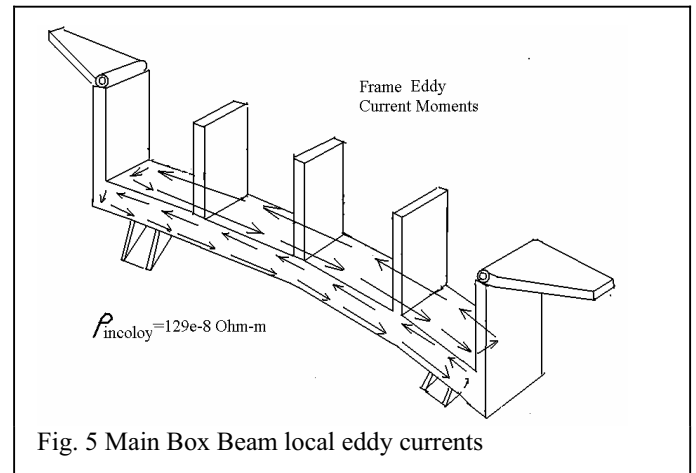


Fig. 5 Main Box Beam local eddy currents

which look structurally like bellows, are electrically resistive compared which the much heavier construction of the sectors themselves. So practically all of the 800 V is dropped across the 32 > sector joints. That is, 25V per joint. There is only a short, low resistance vertical frame leg between the resistive earths at each end of the frame. The current split between the end resistive earths will be driven by the resistance of the straps.

For a 3 milliohm resistive connection between the poloidal limiter and the antenna at each end, a current of up to 17 kA would be generated. To put this in

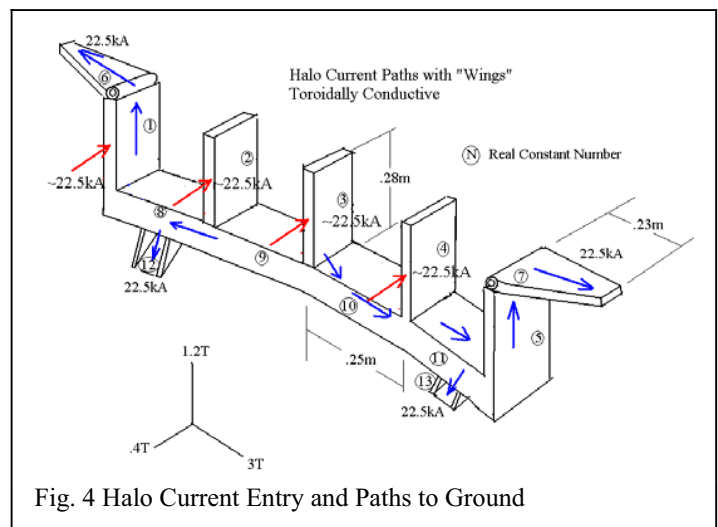


Fig. 4 Halo Current Entry and Paths to Ground

perspective, this must be compared with a total halo current of 90 kA. The additional 17 kA is significant but should not be sufficient on its own to require any drastic change to the design. On JET's A2 ICRF Antennas there are so called 'protection rails' bridging the poloidal limiters which act in the same way. They have resistive connections to the limiters and the measured currents in them were as predicted using the same approach as for the TAE antennas.

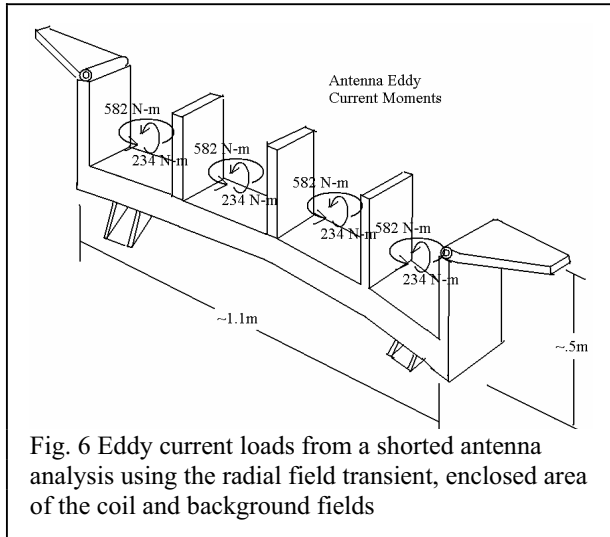


Fig. 6 Eddy current loads from a shorted antenna analysis using the radial field transient, enclosed area of the coil and background fields

II LOAD CALCULATIONS

Conservative estimates of the disruption currents in the TAE antennas and frame were used to calculate loading and resulting stress in the antenna structure. The simplest of a number of methods to compute disruption eddy currents was used. The change in flux multiplied by areas enclosed by frame loops or loops formed in plates is equated with the resistive voltage to compute a current. Currents are then crossed with fields to get Lorentz Forces. Halo current loads were calculated and added to the loads from the toroidal currents in an Excel spreadsheet.

A more rigorous method of calculating loads is a full electromagnetic simulation of the disruption. This was done for the C-Mod MHD antenna.[13]. The electromagnetic solution includes the effects of self inductance and coupling with the plasma and other structures.

Fields, field transients, and halo current specifications were provided by JET[3,12]. Antenna eddy currents were computed assuming the antenna is shorted. In the latest design, frame forces primarily result from halo currents entering around the mini limiters that now protect the antenna windings. Accelerations due to the vessel disruption dynamic response were included in the loading. These are small compared with Lorentz loads. Some dynamic calculations have been performed, but due to the

complexity of the attachment system. The dynamic response is uncertain, and a conservative design is called for, and provided for, in the assumptions regarding the loading. Initially, due to the logistics of implementing the evolving loads, the more conservative loading based on downward current flow, is retained in some of the calculations where analysis consistent with the optimal loading only would serve to demonstrate more margin. Loading is based on use of the resistive straps. Two cases are considered. One with an equal set of resistive straps, and another with 2mOhm straps used at the wings, and 3 mOhm used at the feet. The model is regionalized and sections are tracked via real constant numbers. Total loads per real constant are applied as nodal forces computed from the total section load divided by the number of nodes in the section. There were a couple of resistive earth load cases. In one treatment of the halo currents, the distribution entering the top and bottom and exiting top and bottom were assumed equal. For straps which are 2mOhm across the wings and 3 mOhms across the feet, 27kA exits in the wings and 18 kA exits at the feet.

III ANALYTIC MODELS

ANSYS is used for the solution phase of the analysis. The model is built in a code outside of ANSYS. In this code, loads can be applied as nodal loads computed from spreadsheet treatment of the currents and fields, or fields and currents in the various components can be specified and loads computed. The spread sheet calculations were used in the latest models, for the earlier models the frame current was input to the frame elements by dividing the currents uniformly to the number of elements in the cross section of the frame tube. Nodal Lorentz forces were computed from specified fields and currents using an

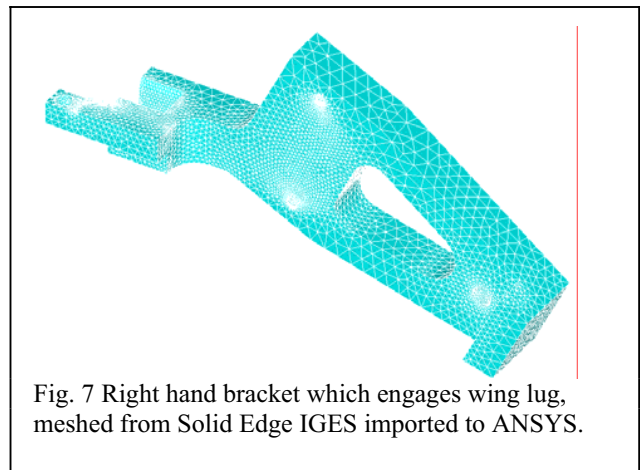


Fig. 7 Right hand bracket which engages wing lug, meshed from Solid Edge IGES imported to ANSYS.

Excel spreadsheet. The model, with loading was then transferred to ANSYS for the structural solution. For some of the detailed parts, geometry could be extracted from the Solid Edge model and imported into ANSYS. Only a few of the parts for which this conversion was

attempted, were fully merged solid volumes. Figure 7 shows a part which could be analyzed in this way. Static and dynamic solutions were used. The dynamic response of the antenna and frame is computed using a time transient analysis with the loading assumed as half a sine wave. Dynamic solutions were not attempted for every evolution of the design, but were used to establish dynamic load factors (DLF) to apply to static analyses.

IV STRESS RESULTS

IV.A. Frame Stresses

The results reported here are for the antenna and its structure and do not include the effect of the attachment loads on the saddle coil and poloidal limiter. These structures should be separately qualified. Effects of thermal loads on the mini-limiters have not been

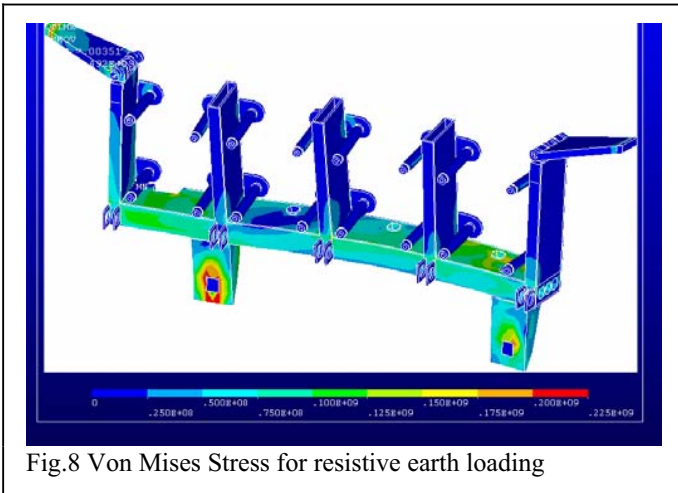


Fig.8 Von Mises Stress for resistive earth loading

considered. The frame Von Mises Stress is shown in figure 8. In this plot loading is for currents based on 2 mOhm/3mOhm resistive earths, at upper and lower attachment points. The plotted stress range peaks at 225 MPa (248 MPa with a 1.1 DLF). In this view there is only a tiny area at the lower attachment with stresses above this. These stresses should be compared with the bending

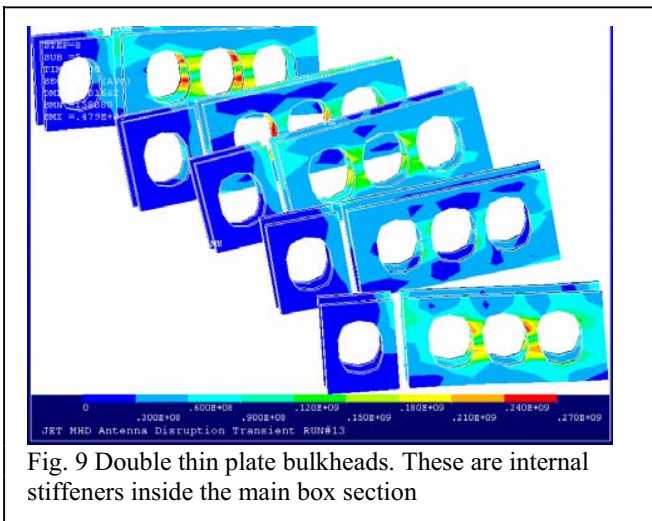


Fig. 9 Double thin plate bulkheads. These are internal stiffeners inside the main box section

allowable. If the plate is not solution annealed but annealed it will have a yield and bending allowable of 447 MPa. Other areas with significant stresses are the notch on the back side of the box beam (left rear in figure 8), holes in the box beam for the antenna leads – particularly near the lower attachment brackets, and the holes in the internal box stiffeners (Fig. 9). The peak stress in the thin section of the bulkhead plates is 270 MPa. These results are from the dynamic model at the time of peak stress in these components. Loading was from the equal resistive earth load case. These are 5mm thick. The solid bulkhead would have lower stress, but would weigh more. The bending allowable for the annealed 625 material is 447 MPa.

IV.B. Remotely Operated Clamp

The poloidal limiter clamp is loaded with 10000N (2248lb) wing lug reaction force plus the clamping forces applied during installation. This was calculated from ANSYS reaction forces from the model shown in figure 1, and additional hand calculations. The inner cylinder had been thinned to reduce the weight for ease of remote handling. This was a source of higher stress, and has been improved in the final design.

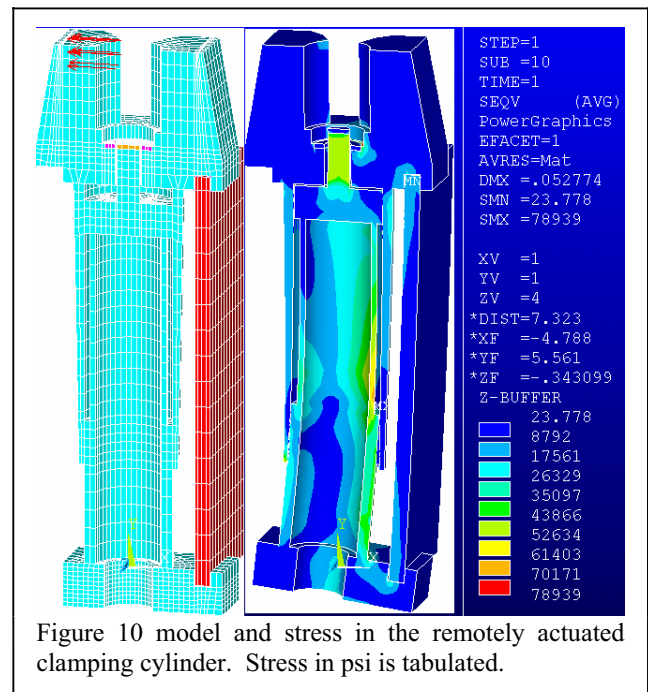


Figure 10 model and stress in the remotely actuated clamping cylinder. Stress in psi is tabulated.

IV.C. Antenna Wire and Ceramic Spoolpiece

The antenna wire support spoolpiece has had many analysis iterations. As of April 2004, the spoolpiece is made up from ceramic disks stacked on a one cm central rod. No preload is intended, and the behavior of the stack with frame imposed displacements, and antenna loads

applied, is non-linear. Edge compressive loads are mitigated by radiusing the edges of the stacked disks. The local stress in the disks without the radius is shown in figure 11. The model of the spoolpiece stack is shown in figure 10. 718 wire is specified for the antenna wire. A

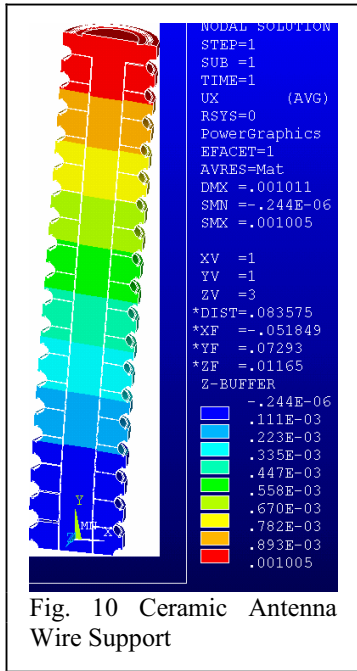


Fig. 10 Ceramic Antenna Wire Support

while conservative loading has been used, loading remains uncertain, and conservative design is called for.

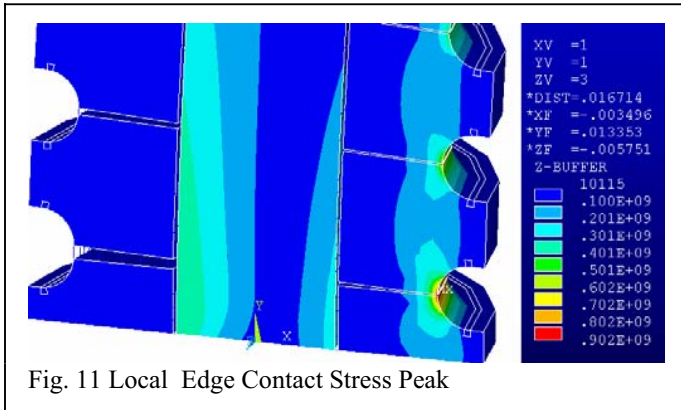


Fig. 11 Local Edge Contact Stress Peak

In general if the better grades of material are selected for components, the antenna will satisfy the design criteria with adequate margins to accommodate the uncertainties. Work hardened versions of Inconel 625 were recommended for the frame structure, but annealed (but not solution annealed) properties are also acceptable. Nimonic bolts are specified for the attachment points and have very good properties at the expected 350 C operating temperature. Ceramic washers at the lower support details should be aluminum oxide, at least 2 cm OD . 718 wire is specified for the antenna wire. Use of 718 wire for the antennas provides fore a robust design. The antenna

frame is highly loaded, and larger sections could be used throughout, however. keeping weight down helps with

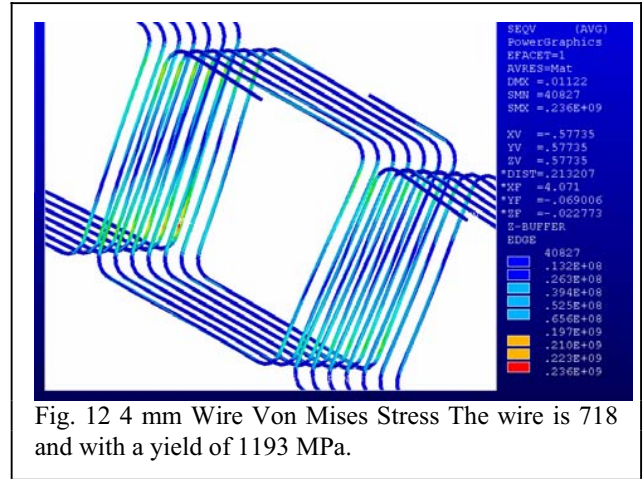


Fig. 12 4 mm Wire Von Mises Stress The wire is 718 and with a yield of 1193 MPa.

remote handling, and high strength materials have been specified over increasing section thicknesses. The bulkhead plates are acceptable without the cold-worked material at the thin webs. The holes in the main beam are acceptable also but these are an area where higher yield material would be used to advantage. Reinforcement pads at the holes were tried to reduce the local stress but they didn't help.

REFERENCES

- [1] "The new TAE - Alfvén Wave Active Excitation System at JET", D.Testa, A.Fasoli, et. al., 23rd Symposium on Fusion Technology,SOFT, Sept 20-24, 2004
- [2] Fusion Ignition Research Experiment Structural Design Criteria; Doc. No. 11_FIRE - DesCrit_IZ_022499.doc; February, 1999
- [3] Memorandum To D Testa, A Kaye, B Walton, M Way From V Riccardo vricc@jet.uk, 5th February 2003 "HALO CURRENT AND TAE ANTENNAS"
- [4] TAE Antenna KC12 – JET Enhancements – Minutes of Final Design Review Meeting A.Fasoli and D.Testa, Project Leaders, CRPP-EPFL, S.Sanders, Operator Representative, UKAEA JET Facilities, Culham Science Centre, June 10th, 2003.
- [5] Product Literature, Inco Alloys International, Inc Huntington West Virginia 25720, USA Publication # IAI-38 Copyright 1988
- [6] December 10 2003 email from Joe Snipes indicating operating temperature
- [7] Halo current specification from V.Riccardo, dated March 31 2003.
- [8] "Disruption Load Calculations Using ANSYS Transient Electromagnetic Simulations for the Alcator C-Mod Antennas", P. Titus 19th IEEE Symposium on Fusion Engineering, Atlantic City, Jan 21-25, 2002